

Characterization of the thermoluminescence glow curve of $\text{Li}_2\text{B}_4\text{O}_7:\text{Cu,Ag}$

J.F. Benavente^{*}, J.M. Gómez-Ros, V. Correcher

CIEMAT, Av. Complutense 40, E-28040, Madrid, Spain

ARTICLE INFO

Keywords:

Thermoluminescence
Lithium borate
Glow curve analysis
Order of kinetics

ABSTRACT

This work presents the characterization of the thermoluminescence (TL) glow curve of a copper and silver doped lithium tetraborate ($\text{Li}_2\text{B}_4\text{O}_7:\text{Cu,Ag}$) made using three different methods to identify the number of peaks, the trap structure and the kinetics parameters: T_M-T_{stop} , glow curve fitting (GCF) and various heating rates (VHR).

The obtained results can be consistently explained assuming four TL glow peaks in the region 50 - 270 °C, originated by a complex trap structure: continuous energy distributions for peaks I, III and IV, and general order kinetics (GOK) discrete trapping level for peak II. Quite similar activation energy values have been obtained by GCF and VHR methods.

1. Introduction

Lithium based thermoluminescent materials are currently used as passive dosimeters in many radiation dosimetry services (Olko et al., 2006). In addition to LiF phosphors, LiF:Ti,Mg and LiF:Mg,Cu,P (Delgado et al., 1995), suitable for many applications because of their sensitivity, photon tissue equivalence and the possibility of use for mixed field dosimetry using pairs of $^6\text{Li}/^7\text{Li}$ detectors, other detectors based on doped lithium borates (Pekpak et al., 2010) are also used as they show similar advantageous properties, including an increased thermal neutron sensitivity using a ^6Li and ^{10}B enriched material. Moreover, lithium tetraborate ($\text{Li}_2\text{B}_4\text{O}_7$) has an atomic effective atomic number, $Z_{\text{eff}} = 7.39$, very close to human tissue (Pekpak et al., 2010).

Different elements (Ag, Cu, In, Mn, P ...) have been used as dopants in lithium tetraborate (Pekpak et al., 2011). Among them, the doubly doped $\text{Li}_2\text{B}_4\text{O}_7:\text{Cu,Ag}$ exhibited a wide range of TL linear response between 100 mGy and 100 Gy (Patra et al., 2013). Although $\text{Li}_2\text{B}_4\text{O}_7:\text{Cu,Ag}$ has been already studied in terms of synthesis methods, crystalline properties, material characterization (Scanning Electron Microscopy, X-ray diffraction, etc.), and luminescent response (Pekpak et al., 2010, 2011; Patra et al., 2013; Doull et al., 2014; Rawat et al., 2012), its glow curve itself presents a complex structure with three broad apparent peaks whose structure and kinetic properties have not been yet examined in enough detail.

The purpose of this work is to investigate the glow curve structure of $\text{Li}_2\text{B}_4\text{O}_7:\text{Cu,Ag}$ by applying a number of different methods to identify the individual glow peaks and the corresponding trapping levels configuration. In particular, the T_M-T_{stop} method (McKeever, 1985) has been

used to reveal the possible presence of hidden peaks as well as to recognize the appropriate kinetics model according to the shape of the T_M-T_{stop} curve. These results have been used to set the equations for the fitting of the glow curves using a previously developed software (Benavente et al., 2019). Special care has been taken to account that just fitting a glow curve by a given combination of peaks is not enough to identify neither peaks nor kinetics models because different sets of parameters can be fitted to the same curve (Chen and McKeever, 1997). Thus, the combined set of experimental methods described in next section has been used to get consistent results.

2. Materials and methods

Synthetic $\text{Li}_2\text{B}_4\text{O}_7:\text{Cu}_{0.4\%},\text{Ag}_{0.1\%}$ was prepared in the laboratories of the Oklahoma State University Physics Department by combustion method from a solution of LiNO_3 (purity of 99%), H_3BO_3 (99.99%), $\text{C}_2\text{H}_5\text{NO}_2$ (99%), $\text{Cu}(\text{NO}_3)_2 \cdot \text{XH}_2\text{O}$ (99.999%) and AgNO_3 (99%) in deionized water (Doull et al., 2014). The solution was successively prepared in several steps consisting of: (i) stirring at 300 °C till the solution reduces from 600 to 50 ml, (ii) increasing the temperature to 450 °C until combustion, (iii) crushing the sample in a mortar and subsequently annealing at 875 °C for 1 h in an alumina boat crucible, (iv) cooling on a metal plate out of the oven.

The thermoluminescence (TL) measurements have been done using an automated reader model Risø TL DA-12 equipped with an EMI 9635 QA photomultiplier with a blue filter (a Melles-Griot FIB002). The samples have been irradiated with the $^{90}\text{Sr}/^{90}\text{Y}$ source located inside the TL reader, delivering an absorbed dose rate of 0.012 Gy/s. All the

^{*} Corresponding author. CIEMAT, Av. Complutense 40, 28040, Madrid, Spain.
E-mail address: jf.benavente@ciemat.es (J.F. Benavente).

measurements have been made in a N₂ atmosphere.

Three different methods for characterizing the TL emission of Li₂B₄O₇:Cu,Ag and the corresponding kinetic parameters have been used: T_M-T_{stop}, glow curve fitting (GCF) and various heating rates (VHR) (McKeever, 1985; Chen and McKeever, 1997).

The T_M-T_{stop} method (McKeever, 1985) permits to identify the most prominent of the peaks in the glow curve, their kinetic order as well as to distinguish between single discrete peaks and continuous or quasi-continuous distribution of peaks. The method has been applied according to the following sequence: i) reader annealing of the sample followed by irradiation at 100 mGy using the ⁹⁰Sr/⁹⁰Y source and linear heating at 1 °C/s to a temperature T_{stop}; ii) cooling to room temperature and reheat of the sample at 1 °C/s up to 400 °C to register the position of the first maximum, T_M; iii) the procedure has been repeated increasing T_{stop} from 70 °C to 270 °C in steps of 2 °C to obtain the plot of T_M versus T_{stop}.

The TL glow curves have been analysed with a deconvolution program that resolves the individual glow peaks assuming either discrete and continuous distribution of trapping centres as well as first and general order kinetics (GOK). This software is based on a long series of previous works (Delgado and Gómez-Ros, 1990; Gómez-Ros et al., 1999; Kitis and Gómez-Ros, 2000; Gómez-Ros and Kitis, 2002) recently upgraded to improve the capability of considering different kinetic models for the peaks of the same glow curve (Benavente et al., 2019).

The software obtains the best fit of the TL glow curve by a linear combination of peaks using a Levenberg–Marquardt algorithm (Horowitz and Yossian, 1995) to minimise the χ^2 function:

$$\chi^2 = \sum_i \left(I(T_i) - \sum_{n=1}^{N_{\text{peaks}}} I_n(T_i) \right)^2 \quad (1)$$

For the peaks arising from a continuous distribution of trapping centres, either a Gauss or an exponential function can be considered, i.e.:

$$n_{\text{Gauss}}(E) = \frac{n_0}{\sqrt{2\pi\sigma^2}} e^{-\frac{(E-E_0)^2}{2\sigma^2}} \quad (2)$$

$$n_{\text{exp}}(E) = \frac{n_0}{\sigma} e^{-\frac{E-E_0}{\sigma}} \quad (3)$$

The VHR method (Chen and McKeever, 1997) is based on the equation that relates the activation energy, *E*, and the frequency factor, *s*, with the temperature of the maximum, *T_M* of a single first order kinetic glow peak measured at a linear heating rate, *β*:

$$\frac{E}{KT_M} = \frac{s}{\beta} \exp\left(-\frac{E}{KT_M}\right) \quad (4)$$

Thus, the activation energy, *E*, can be obtained from the slope of the linear dependence of log(*s*/T_M²) versus 1/*T_M*. In case of a complex glow curve, the *E_i* values can be obtained from the maximum temperature of fitted glow peaks, *T_{M_i}*, in glow curves measured at different heating rates, thus comparing these values with the fitted ones to check the consistency to check for the consistency of the results.

Although the VHR method was developed assuming first order kinetics, the method is a very good approximation in case of general order kinetics (Chen and McKeever, 1997). Moreover, an equation similar to (4) is obtained for a peak arising from a continuous distribution of trapping centres, with an effective activation energy *E_{eff}* replacing the *E* value (Correcher et al., 2017).

3. Results and discussion

The prompt glow curves of Li₂B₄O₇:Cu,Ag samples measured at a linear heating rate of 2 °C/s immediately after irradiation show three main broad peaks centred around 90 °C, 150 °C and 235 °C (Fig. 1). In order to investigate the peak structure before attempting to analyse the whole glow curve by fitting procedures, the T_M-T_{stop} described in

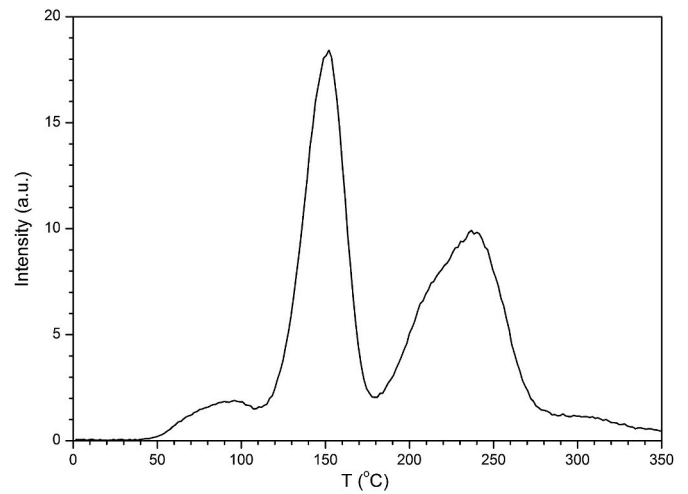


Fig. 1. TL glow curve of Li₂B₄O₇:Cu,Ag measured at a heating rate of 2 °C/s.

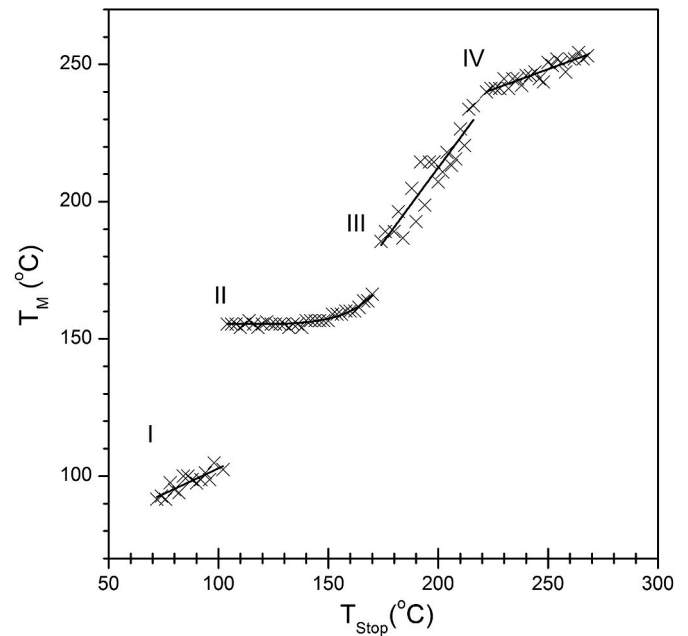


Fig. 2. T_{MAX}-T_{STOP} curve for the TL of Li₂B₄O₇:Cu,Ag in the range 70–270 °C.

previous section has been applied. Fig. 2 shows the first maximum, T_M, obtained when the material is reheated after being irradiated and heated up to T_{stop} in the range 70 °C to 270 °C in steps of 2 °C (McKeever, 1985). As it can be seen, four components can be identified: I) a straight increasing line indicating a continuous distribution of peaks in the region 70-100 °C; II) a straight flat line followed by an increasing tail that is usually indicative of a single general order kinetics peak in the region 100-170 °C; III) another straight increasing line indicating a continuous distribution in the region 170-225 °C; and IV) a last straight increasing line corresponding to a continuous distribution in the region 225-270 °C.

According to the results of the T_M-T_{stop} test, the glow curves of samples irradiated at 100 mGy and recorded with a linear heating rate of 2 °C/s up to 350 °C have been fitted by the combination of four peaks:

$$I_{\text{TL}}(T) = I_i^{(\text{continuous})}(T) + I_{II}^{(\text{GOK})}(T) + I_{III}^{(\text{continuous})}(T) + I_{IV}^{(\text{continuous})}(T) \quad (5)$$

considering both Gaussian (equation (2)) and exponential (Equation (3)) distributions for peaks I, III and IV. In all the cases, a better agreement, i.

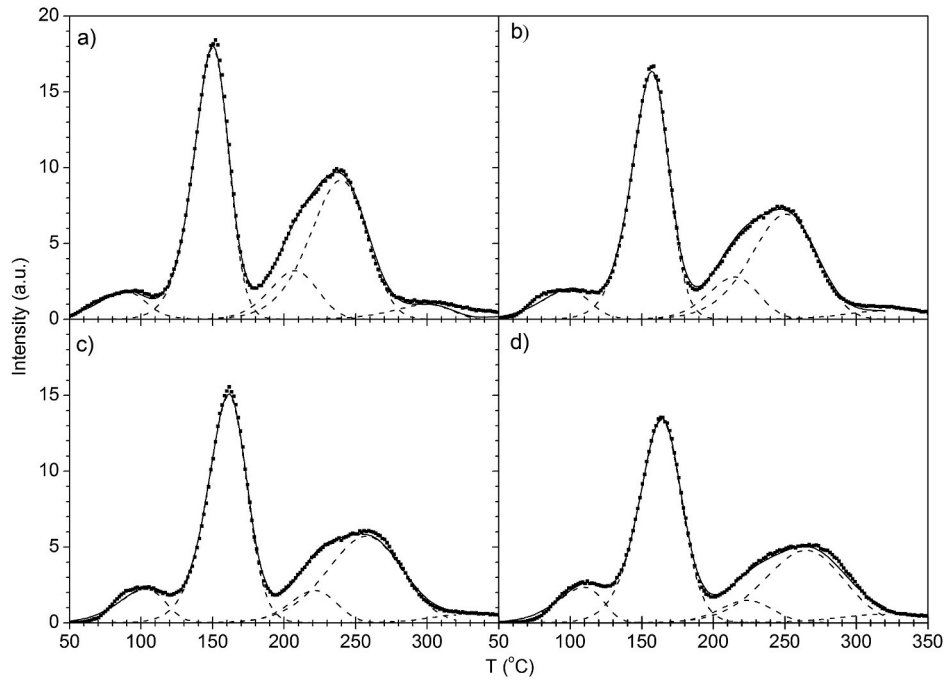


Fig. 3. Glow curve fitting of TL emission of four aliquots, measured at different heating rates: a) $\beta = 2$ °C/s; b) $\beta = 4$ °C/s; c) $\beta = 6$ °C/s; and d) $\beta = 8$ °C/s; showing the experimental glow curves (dots), the fitted curves (solid lines) and the fitted peaks (dashed lines).

e. a lower Figure of Merit (FOM) (Horowitz and Yossian, 1995), has been obtained when an exponential distribution is assumed for peak I and a Gaussian one for peaks III and IV. The presence of an exponential distribution for the lowest temperature peak can be explained as a consequence of the emptying process affecting the shallower levels thus remaining only the deepest exponential tail (Sakurai et al., 2001; Gómez-Ros et al., 2006).

The residual of the fitted curves by equation (5) clearly indicates the presence of some additional contribution in the region above 270 °C. Therefore, a fifth peak has been considered, thus resulting in the following equation:

$$I_{TL}(T) = I_I^{(exp)}(T) + I_{II}^{(GOK)}(T) + I_{III}^{(Gauss)}(T) + I_{IV}^{(Gauss)}(T) + I_V^{(Gauss)}(T) \quad (6)$$

where the fitting equations used for each peak according to the assumed kinetic model are (Benavente et al., 2019):

$$I^{(GOK)} = I_M \exp\left(\frac{E}{KT_M} - \frac{E}{KT}\right) \times \left\{ 1 + \left(\frac{b-1}{b}\right) \frac{E}{K T_M} \int_{T_0}^T \exp\left(\frac{E}{kT_M} - \frac{E}{kT'}\right) dT' \right\}^{-\frac{b}{b-1}} \quad (7)$$

$$I^{(exp)}(T) = \int_{E_0}^{+\infty} s \frac{n_0}{\sigma} \exp\left(-\frac{E-E_0}{\sigma}\right) \times \exp\left(-\frac{E}{KT}\right) \exp\left\{ -\frac{s}{\beta} \int_{T_0}^T \exp\left(-\frac{E}{KT'}\right) dT' \right\} dE \quad (8)$$

$$I^{(Gauss)}(T) = \int_{-\infty}^{+\infty} s \frac{n_0}{\sqrt{2\pi}\sigma^2} \exp\left[-\frac{(E-E_0)^2}{2\sigma^2}\right] \times \exp\left(-\frac{E}{KT}\right) \exp\left\{ -\frac{s}{\beta} \int_{T_0}^T \exp\left(-\frac{E}{KT'}\right) dT' \right\} dE \quad (9)$$

Table 1

Kinetic parameters (T_M , E_0 and σ for continuous distributions; T_M , E and b for GOK) of peaks of $Li_2B_4O_7:Cu,Ag$, obtained by glow curve fitting. The values are the mean ones obtained from 10 aliquots for each considered heating rate.

peak	assumed kinetics	parameter	beta (°C/s)			
			2	4	6	8
I	continuous exponential	T_M (°C)	89	98	102	109
		E_0 (eV)	0.75	0.76	0.79	0.82
		σ (eV)	0.020	0.017	0.014	0.010
II	GOK	T_M (°C)	148	156	161	162
		E (eV)	1.45	1.45	1.42	1.37
		b	1.34	1.34	1.38	1.42
III	continuous gaussian	T_M (°C)	208	216	220	225
		E_0 (eV)	1.61	1.59	1.70	1.68
		σ (eV)	0.043	0.043	0.039	0.043
IV	continuous gaussian	T_M (°C)	240	250	256	264
		E_0 (eV)	1.36	1.28	1.29	1.28
		σ (eV)	0.030	0.038	0.042	0.044

For equations (8) and (9), the maximum condition $dl(T)/dT = 0$ does not permit to explicitly calculate T_M and I_M . Therefore, both quantities are directly obtained from the fitted individual peak.

Fig. 3 shows the glow curves of four samples irradiated at 100 mGy and measured at heating rates 2, 4, 6, 8 °C/s, fitted by equation (6). The measurements have been repeated with 10 aliquots for each heating rate (40 in total) to obtain the mean values of the fitted kinetic parameters corresponding to every glow peak and heating rate: (T_M , E_0 , σ) for continuous distributions, (T_M , E and b) for the general order kinetics peak (Benavente et al., 2019). In all cases, a FOM lower than 3% has been obtained that can be considered a good fit for experimental data. Moreover, the standard deviation of the mean fitted parameters (BIPM, 2008) is always lower than 4,50%.

The results are summarized in Table 1. As it can be expected (Chen and McKeever, 1997), a gradual increase of the temperature of the maxima, T_M , has been obtained when faster heating rates have been applied. Thus, these T_M values have been used to obtain the activation energy (E in case of discrete trap, E_{eff} in case of continuous distributions)

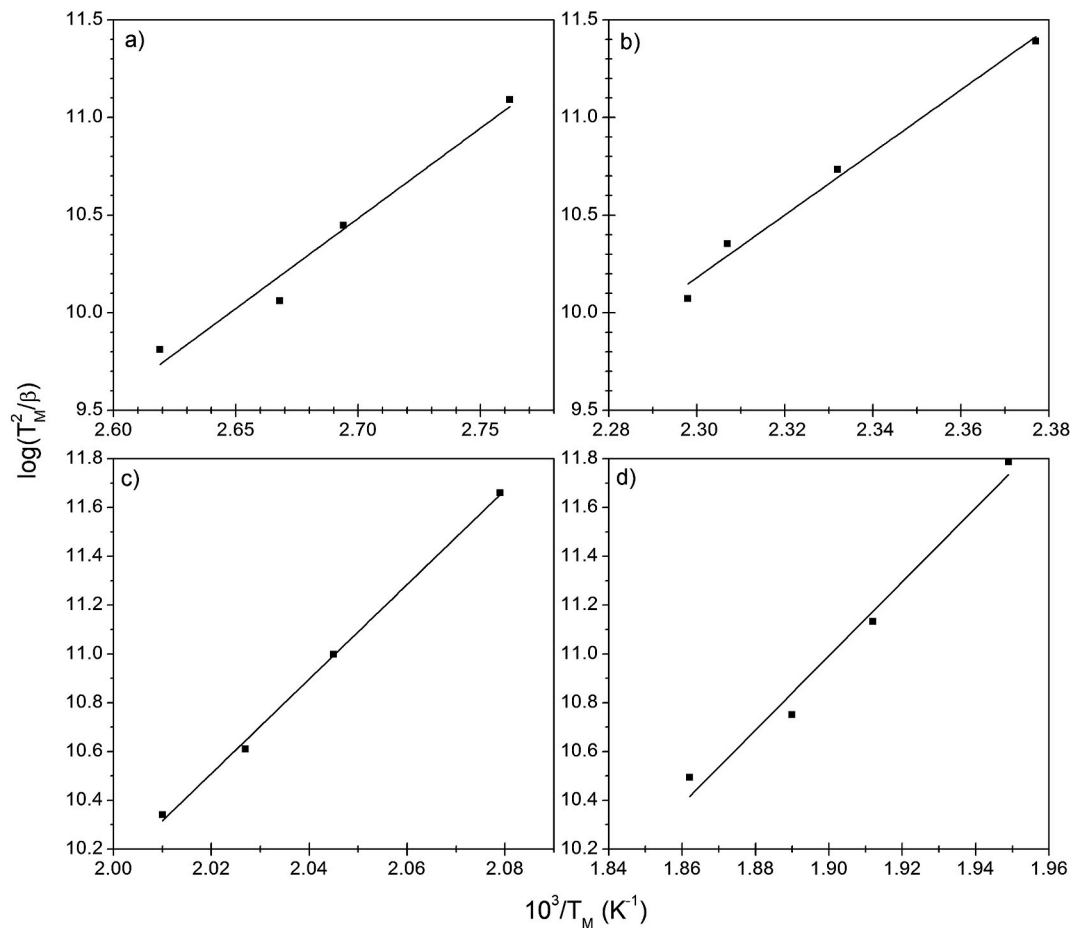


Fig. 4. VHR method results: plot of $-\log(\beta/T_M^2)$ vs. $10^3/T_M$, for peaks I, II, III, IV (respectively figures a, b, c, d). Dots correspond to the mean values obtained from 10 aliquots for each of the four considered heating rates ($\beta = 2, 4, 6, 8$ °C/s).

Table 2

Comparison of activation energy of peaks of $\text{Li}_2\text{B}_4\text{O}_7\text{:Cu,Ag}$, obtained by glow curve fitting and VHR method.

peak	assumed kinetics	GC fitted parameters			VHR
		E (eV)	E_0 (eV)	σ (eV)	E (eV)
I	exponential	–	0.78	0.015	0.80 (0.09)
II	GOK	1.42	–	–	1.38 (0.11)
III	Gaussian	–	1.64	0.042	1.67 (0.05)
IV	Gaussian	–	1.30	0.038	1.31 (0.13)

using the VHR method described in section 2. Fig. 4 plots the values of $-\log(\beta/T_M^2)$ vs. $10^3/T_M$ for heating rates 2, 4, 6, 8 °C and peaks I, II, III, IV (respectively Fig. 4a–d) together with the corresponding linear fitting (correlation coefficient $R \approx 1.0$), whose slope is E/K , being K the Boltzmann's constant.

Table 2 compare the activation energy values obtained by fitting the glow curves (mean values) with those obtained using the VHR method. As it can be seen, the values are consistent in all the cases, even for peaks I, III and IV arising from a continuous distribution of traps. This is not surprising because the fitted σ value indicates a narrow exponential energy distribution for peak I (0.78–0.84 eV approximately) and an effective activation energy, E_{eff} , similar to the energy of the maximum, E_0 , can be expected in case of symmetric energy Gaussian distributions for peaks III and IV.

In summary, the structure of $\text{Li}_2\text{B}_4\text{O}_7\text{:Cu,Ag}$ glow curve up to 270 °C can be consistently explained in terms of four peaks with maximum temperatures around 90 °C, 150 °C, 210 °C and 240 °C for a heating rate

of 2 °C/s. The first peak (I) seems to arise from a narrow exponential distribution of trapping centres with activation energy between 0.78 and 0.80, which agrees with a previous reported value (Rawat et al., 2012.) for this peak. The peak II behaves according to general order kinetics with activation energy 1.4 eV (obtained both by GCF and VHR methods). The peaks III and IV are due to continuous Gaussian distributions centred at energies 1.6 and 1.3 eV respectively (also obtained by GCF and VHR methods).

4. Conclusion

The TL glow curve emission of $\text{Li}_2\text{B}_4\text{O}_7\text{:Cu,Ag}$ has been studied using three methods: T_M - T_{stop} , GCF and VHR, to identify the number of peaks, the possible trap structure and the corresponding kinetics parameters. The structure of the glow curve assumed for the fitting process have been inferred from the T_M - T_{stop} measurements. Then, consistent results have been obtained that permitted to identify four components from 50 to 270 °C originated by a complex trap structure: continuous energy distributions for peaks I, III and IV, and GOK discrete trapping level for peak II. The obtained exponential energy distribution for peak I a consequence of the thermal emptying of the shallower levels at room temperature, already found in some materials (Sakurai et al., 2001; Gómez-Ros et al., 2006).

In particular, the activation energy values obtained by GCF and VHR agree pretty well within the uncertainty of the measurements thus confirming the possibility of extending the use of the VHR method beyond the case of single trap first order kinetics (Chen and McKeever, 1997; Correcher et al., 2017).

The fitting residuals indicate the presence of glow peaks at

temperatures higher than 300 °C. Although this contribution has not been studied in this work, it has been considered in fitting equation (6). The results confirmed it does not significantly affect closer peak IV because of the weak overlapping.

Declaration of competing interest

The authors declare that they have no known competing financial interests or personal relationships that could have appeared to influence the work reported in this paper.

Acknowledgements

The authors wish to thank the Department of Physics of the Oklahoma State University for providing the samples of the TL material.

References

- Benavente, J.F., Gómez-Ros, J.M., Romero, A.M., 2019. Thermoluminescence glow curve deconvolution for discrete and continuous trap distributions. *Appl. Radiat. Isot.* 153, 108843.
- Bipm, 2008. Evaluation of measurement data - guide to the expression of uncertainty in measurement (GUM). Report JCGM 100, 2008.
- Chen, R., McKeever, S.W.S., 1997. *Theory of Thermoluminescence and Related Phenomena*. World Scientific Publishing, Singapore.
- Correcher, V., Gomez-Ros, J.M., Dogan, T., Garcia-Guinea, J., Topaksu, M., 2017. Optical, spectral and thermal properties of natural pumice glass. *Radiat. Phys. Chem.* 130, 69–75.
- Delgado, A., Gómez-Ros, J.M., 1990. Evolution of TLD-100 glow peaks IV and V at elevated ambient temperatures. *J. Phys. D Appl. Phys.* 23, 571–574.
- Delgado, A., Sáez-Vergara, J.C., Gómez-Ros, J.M., Romero, A.M., 1995. Intrinsic self-dosing and long-term stability of LiF TLD-100 and GR-200 TL detectors. *Radiat. Protect. Dosim.* 58, 211–216.
- Doull, B.A., Oliveira, L.C., Wang, D.Y., Milliken, E.D., Yukihara, E.G., 2014. Thermoluminescent properties of lithium borate, magnesium borate and calcium sulfate developed for temperature sensing. *J. Lumin.* 146, 408–417.
- Gómez-Ros, J.M., Kitis, G., 2002. Computerised glow curve deconvolution using general and mixed order kinetics. *Radiat. Protect. Dosim.* 101, 47–52.
- Gómez-Ros, J.M., Sáez, J.C., Romero, A.M., Budzanowski, M., 1999. Fast automatic glow curve deconvolution of LiF:Mg,Cu,P curves and its application in routine dosimetry. *Radiat. Protect. Dosim.* 85, 249–252.
- Gómez-Ros, J.M., Correcher, V., García-Guinea, J., Delgado, A., 2006. Evolution of the trapped charge distribution due to trap emptying processes in a natural aluminosilicate. *Radiat. Protect. Dosim.* 119, 93–97.
- Horowitz, Y.S., Yossian, D., 1995. Computerised glow curve deconvolution: application to thermoluminescence dosimetry. *Radiat. Protect. Dosim.* 60.
- Kitis, G., Gómez-Ros, J.M., 2000. Thermoluminescence glow curve deconvolution functions for mixed order kinetics and continuous trap distribution. *Nucl. Instrum. Methods A* 440, 224–231.
- McKeever, S.W.S., 1985. *Thermoluminescence of Solids*. Cambridge University Press, London.
- Olko, P., Currihan, L., van Dijk, J.W.E., López, M.A., Wernli, C., 2006. Thermoluminescent detectors applied in individual monitoring of radiation workers in Europe - a review based on the EURADOS questionnaire. *Radiat. Protect. Dosim.* 120, 298–302.
- Patra, G.D., Singh, S.G., Tiwari, B., Sen, S., Desai, D.G., Gadkari, S.C., 2013. Thermally stimulated luminescence process in copper and silver co-doped lithium tetraborate single crystals and its implication to dosimetry. *J. Lumin.* 137, 28–31.
- Pekpak, E., Yilmaz, A., Özbayoglu, G., 2010. An overview on preparation and tl characterization of lithium borates for dosimetric use. *Open Miner. Process. J.* 3, 14–24, 2010.
- Pekpak, E., Yilmaz, A., Özbayoglu, G., 2011. The effect of synthesis and doping procedures on thermoluminescent response of lithium tetraborate. *J. Alloys Compd.* 509, 2466–2472.
- Rawat, N.S., Kulkarni, M.S., Tyagi, M., Ratna, P., Mishra, D.R., Singh, S.G., Tiwari, B., Soni, A., Gadkari, S.C., Gupta, S.K., 2012. TL and OSL studies on lithium borate single crystals doped with Cu and Ag. *J. Lumin.* 132, 1969–1975.
- Sakurai, T., Shoji, K., Itoh, K., Gartia, R.K., 2001. Origin of the exponential distribution of traps in glass. *J. Appl. Phys.* 89, 2208–2212.